Research Article | Vol. 11, No. 8 / 1 August 2020 / Biomedical Optics Express 4431
Biomedical Optics EXPRESS

Frequency-doubled femtosecond Er-doped fiber laser for two-photon excited fluorescence imaging

DOROTA STACHOWIAK,[1,3] JAKUB BOGUSŁAWSKI,[2,3] ALEKSANDER GŁUSZEK,[1] ZBIGNIEW ŁASZCZYCH,[1] MACIEJ WOJTKOWSKI,[2] AND GRZEGORZ SOBOŃ[1,*]

[1]*Laser & Fiber Electronics Group, Faculty of Electronics, Wrocław University of Science and Technology, Wybrzeze Wyspianskiego 27, 50-370 Wroclaw, Poland*
[2]*International Centre for Translational Eye Research, Institute of Physical Chemistry, Polish Academy of Sciences, Kasprzaka 44/52, 01-224 Warsaw, Poland*
[3]*These Authors contributed equally to this work*
[*]*grzegorz.sobon@pwr.edu.pl*

Abstract: A femtosecond frequency-doubled erbium-doped fiber laser with an adjustable pulse repetition rate is developed and applied in two-photon excited fluorescence microscopy. The all-fiber laser system provides the fundamental pulse at 1560 nm wavelength with 22 fs duration for the second harmonic generation, resulting in 1.35 nJ, 60 fs pulses at 780 nm. The repetition rate is adjusted by a pulse picker unit built-in within the amplifier chain, directly providing transform-limited pulses for any chosen repetition rate between 1 and 12 MHz. We employed the laser source to drive a scanning two-photon excited fluorescence microscope for *ex vivo* rat skin and other samples' imaging at various pulse repetition rates. Due to compactness, ease of operation, and suitable pulse characteristics, the laser source can be considered as an attractive alternative for Ti:Sapphire laser in biomedical imaging.

1. Introduction

Femtosecond lasers are the enabling technology in the field of biophotonics, including non-invasive diagnostics, optical imaging, and multiphoton microscopy (MPM) [1,2]. In the latter group, two-photon excited fluorescence (TPEF) – a process in which two photons are absorbed simultaneously by a single fluorophore – is an important example of such a technique [3]. Currently, state-of-art TPEF imaging systems primarily utilize commercially-available femtosecond Ti:Sapphire lasers delivering femtosecond pulses in the 700-1000 nm window [4–7]. However, due to their architecture, Ti:Sapphire lasers have certain disadvantages hindering, or in many cases prohibiting real-life applications outside the laser physics laboratory. A Ti:Sapphire laser is based on a free-space resonator pumped by an expensive green laser (532 nm), besides active water cooling and an optical table are often required. As a result, the entire setup becomes complex, bulky, and expensive. Working with Ti:Sapphire lasers might be bothersome since they often require re-alignment or some adjustments to initiate a pulsed operation. Considering real-life applications in biological or medical research laboratories, clinics, and hospitals, the TPEF imaging system should be as simple as possible, while daily operation of a Ti:Sapphire laser requires knowledge about laser optics. Moreover, intrinsically Ti:Sapphire lasers operate at relatively high pulse repetition frequencies (f_{rep}), often above 70 MHz. However, some applications require much lower f_{rep}, which implies using an external pulse-picker (based on a bulk crystal) to reduce the repetition rate. A pulse-picker introduces unwanted chromatic dispersion and further increases the size, cost, and complexity of the setup.

#396878 https://doi.org/10.1364/BOE.396878
Journal © 2020 Received 4 May 2020; revised 10 Jul 2020; accepted 12 Jul 2020; published 20 Jul 2020

Biomedical Optics EXPRESS

The development of femtosecond lasers is often driven by the needs of particular applications in biology and medicine. One such example is a need for low and adjustable f_{rep} femtosecond sources, especially important for multiphoton microscopy. It has been shown that reducing the pulse f_{rep} is beneficial for increasing the TPEF signal during the imaging of biological tissues. One example is the imaging of skin and a few other pigment-containing tissues, where thermal-mechanical damage can be mitigated by using a pulse picker [8]. The origin of this damage is strong one-photon absorption of melanin at the wavelength of excitation [9]. For this reason, the average excitation power cannot be increased, as this will result in tissue damage. On the contrary, while picking pulses, the average laser power is reduced, but the peak power is maintained. Moreover, it also allows sufficient time for heat dissipation between pulses. As a consequence, when allowed by biochemical damage threshold, it gives room to increase further the pulse peak power resulting in increased TPEF signal [10]. This has also been exploited in deep-tissue brain imaging, where the optimal repetition rate was determined to be within 1 and 10 MHz [11]. The optimal repetition rate depends on imaging depth, highlighting the need for an arbitrarily tunable source. In another example, it was shown that reduced f_{rep} increases fluorescence yield through dark state relaxation. Increasing time between pulses to >1 μs ensures that transient molecular dark states with a long lifetime will relax between two absorption events [12]. Finally, pulse pickers are commonly used in two-photon fluorescence lifetime imaging microscopy (FLIM) to adjust the pulse separation to the specific fluorophore's lifetime [13–15]. For those reasons, the ability to reduce and control the repetition rate is very important.

Currently, there is a demand for compact lasers with ultrashort pulse duration, but not necessarily high average power, especially in *in vivo* imaging of, e.g., human retina. As an alternative to Ti:Sapphire lasers, compact frequency-doubled Erbium-doped fiber lasers can be used [16]. Fiber lasers, compared to solid-state Ti:Sapphire lasers, are more compact and simple, robust, maintenance-free, and cost-effective. However, achieving few-cycle pulses directly from Erbium-fiber oscillators is challenging. Sub-50 fs pulses were obtained from the setup utilizing free space optics [17], while in the case of all-fiber Erbium-lasers, pulse duration was limited to ~50 fs by high order dispersion and nonlinear effects in optical fibers [18,19]. Another approach to achieve fs pulses is external amplification and compression, using non-standard fibers with precisely adjusted length, which allows to achieve even sub-20 fs pulses [20–24]. The pulse duration of 14 fs was achieved from an amplified carbon nanotube mode-locked fiber laser; however, the setup includes at its output a highly nonlinear fiber (HNLF) and a prism pair [25]. Generation of 22.7 fs pulses with 2.8 nJ energy was reported in [26], by single-stage soliton compression using a standard single-mode fiber (SMF) for both pre-stretching pulses from the oscillator, and their compression after amplification. All-fiber and polarization-maintaining (PM) setup presented in [27] allowed to achieve 24 fs pulses with the energy of 3 nJ. The presented setup utilizes only three commercially available PM fiber optic components and two types of PM fibers (also commercially available – SMF and active fiber), providing linear polarization of the output pulses and stable operation. Further power scaling is possible by using conventional chirped pulse amplification (CPA) scheme, in which the seed pulses are stretched, amplified, and finally compressed in a linear compressor (e.g., based on diffraction gratings). Such an approach enables amplification even to μJ energy levels and MW/GW peak powers [28–30], but for the cost of the dramatically increased complexity of the system and significantly longer output pulse (>400 fs), which is too long for *in vivo* TPEF imaging of delicate biological tissues.

Femtosecond pulses at 1560 nm wavelength can be converted to ultrashort 780 nm pulses, to ideally match the two-photon absorption spectra of many fluorophores of interest, by adding a frequency-doubling stage for the second harmonic generation (SHG). As an example, a high-power frequency-doubled laser with 520 fs pulses at 85 MHz repetition rate, resulting in pulse energy of 10.3 nJ and peak power of more than 19.8 kW was used for in-vivo TPEF spectroscopy and imagining [31]. However, the relatively long pulse duration and high repetition rate exclude such

Biomedical Optics EXPRESS

sources from, e.g., retinal imaging [4]. Another system for two-photon microscopy, generating 191 fs pulses with a 156 MHz repetition rate and 1 W of average power, was demonstrated in [32]. The generation of much shorter pulses - about 40 fs at 796 nm was presented in [33], which was achieved by converting 50 fs pulses at the central wavelength of 1600 nm by the SHG module. The average power of the signal at ~800 nm was 140 mW, corresponding to 3.5 nJ pulse energy at a f_{rep} of 40 MHz. The system does not contain any f_{rep} control and requires three amplification stages. Moreover, configuration based on nonlinear frequency conversion creates a possibility for dual-wavelength operation for simultaneous two- and three-photon imaging in a multimodal instrument. In [34], 80 fs pulses at 790 nm wavelength (61 mW of average power) were generated and used simultaneously with residual, unconverted 80 fs pulses at 1580 nm (117 mW of average power). The residual 1580 nm pulses were used for third-harmonic generation (THG) skin imaging, while 790 nm pulses for TPEF and SHG imaging. However, none of the configurations presented so far has provided an adjustable f_{rep}, required in many biomedical applications.

In this work, we report a frequency-doubled Er-fiber laser system for TPEF imaging, which addresses the main shortcoming of the previously reported setups: it enables pulse repetition rate tuning by means of a fiber-coupled pulse-picker integrated with the amplifier chain. The system delivers sub-65 fs pulses with >1.3 nJ energy preserved in the entire f_{rep} tuning range. The applicability of the source for two-photon excited fluorescence microscopy was confirmed by imaging of *ex vivo* samples at various pulse repetition rates. We show that reducing the pulse repetition rate allows us to increase fluorescence intensity from rat skin samples.

2. Design of the frequency-doubled Er-fiber laser source

Figure 1 shows the experimental setup of the frequency-doubled Er-doped fiber laser source. As a seed source, a ring cavity Er-doped fiber laser (EDFL) mode-locked via semiconductor saturable absorber mirror (SESAM) was used (Batop GmbH). The seed generated 325-fs pulses at a 35.7 MHz repetition rate and average power of 1.1 mW at 1561 nm central wavelength. Next, the pulses were pre-amplified in an in-house made Erbium-doped fiber amplifier (EDFA) based on a 1.5 m-long segment of highly-Erbium doped fiber (Liekki Er80-4/125-PM, EDF). After amplification, the pulses entered a pulse-picker (PP) based on a fast acousto-optic modulator (Gooch & Housego Fibre-Q 200 MHz, AOM). The details on the PP design were already presented in our previous work [35]. After f_{rep} reduction, the pulses were amplified in a final amplification stage, based on the same 1.5 m-long EDF as in the previous stage. An additional band-pass filter (BPF) with 10 nm width (centered at 1560 nm) was placed before the power amplifier (PMBP-1560-10-2-B-Q-2-C, Advanced Fiber Resources). The BPF limited the spectral width prior amplification and enabled achieving a clean pulse shape at the output, with minimized sidebands (the role of the BPF is explained later in the text).

The setup was entirely fiberized and spliced using a standard arc-fusion splicer. All fibers and components used in this setup were single-mode and polarization-maintaining (PM-SMF), providing polarization stability, which is crucial for frequency doubling. The entire system was built using only two types of fibers (the EDF and PM-SMF). All components are standard, off-the-shelf PM fiber components (Advanced Fiber Resources).

The source is capable of generating pulses with duration down to 22 fs at any chosen repetition rate from 1 to 12 MHz. The evolution of the optical spectrum and pulse shape in the system is depicted in Fig. 2. The optical spectra (recorded with an optical spectrum analyzer, Yokogawa AQ6370B, OSA) and autocorrelation traces (APE PulseCheck) were measured at three different stages of the setup and the pulse picker frequency set to 1 MHz: after the seed oscillator, i.e. before entering the preamplifier (a,b), after the preamplifier and AOM (c,d), and after the BPF (e,f). The spectrum after the second amplifier is depicted in Fig. 3(a). It can be seen that the relatively narrow spectrum from the seed (a) is significantly broadened during amplification via

Biomedical Optics EXPRESS

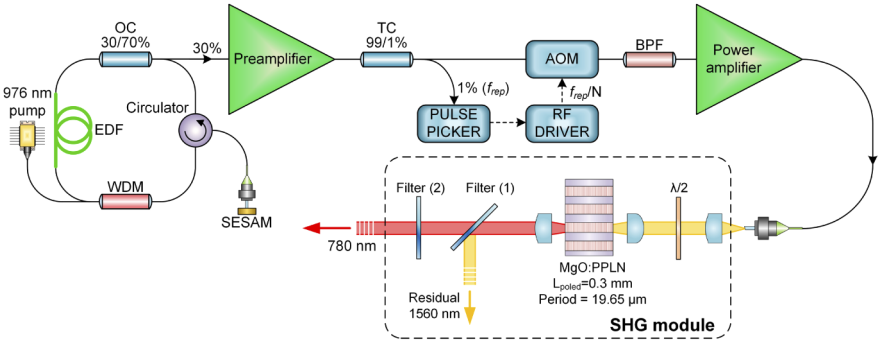

Fig. 1. Scheme of the frequency-doubled, fiber laser: EDF – Erbium-doped fiber; OC – 70/30% output coupler; WDM – 980/1550 nm wavelength division multiplexer; SESAM - semiconductor saturable absorber mirror; TC – 99/1% tap coupler; AOM – 200 MHz acousto-optic modulator; BPF – 10 nm band-pass filter.

nonlinear effects, mostly self-phase modulation (SPM) [36,37]. The pulse propagation can be described by an interplay of SPM, gain narrowing, second-order and higher-order dispersion [38]. Due to the normal dispersion of the EDF, the pulses experience parabolic amplification [25] and are positively chirped. After the gain fiber, the pulse propagates through a segment PM-SMF with anomalous dispersion; therefore it is again compressed, which results in a 225 fs pulse recorded after the AOM (d). Due to the broad spectrum, the pulse duration after amplification is shorter than generated from the oscillator. Next, the spectrum is intentionally limited to 10 nm using a BPF (e). Spectral narrowing leads to significant elongation of the pulse (f). Such pulse is then amplified in the second amplification stage, where again SPM co-exists with normal dispersion, leading to significant spectral broadening [Fig. 3(a)], which enables compression down to 22 fs [Fig. 3(b)]. Achievement of a pedestal-free, nearly transform-limited pulse at the output of the system was possible due to the use of spectral filtering (i.e. BPF) prior amplification. This is

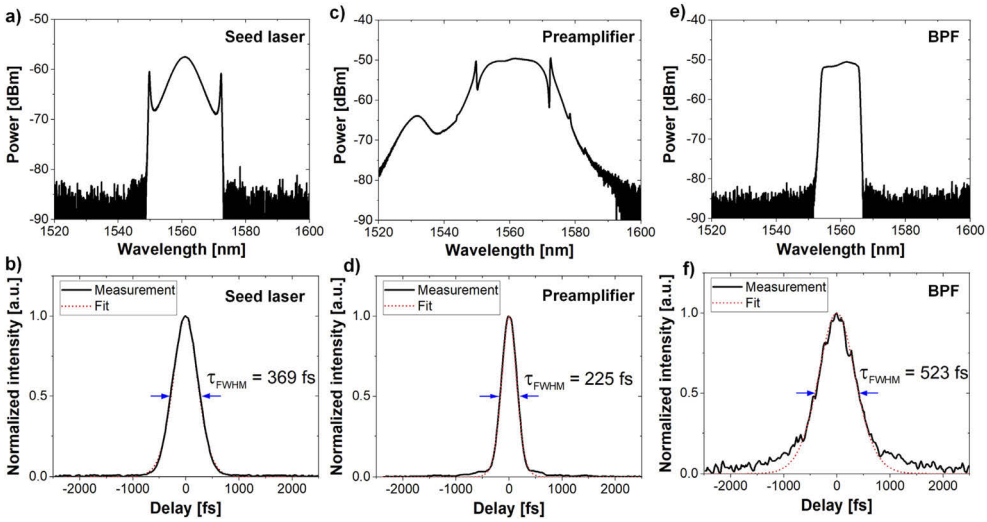

Fig. 2. Evolution of the optical spectrum and pulse shape in the system: spectrum and autocorrelation traces recorded after the seed laser (a,b), preamplifier with the AOM (c,d), and the bandpass filter (e,f).

Biomedical Optics EXPRESS

related to the amount of accumulated nonlinear phase (described by the B integral [37]). It has been shown that gain narrowing in fiber amplifiers leads to a spectral shaping, which degrades the pulse shape [39]. Pre-compensation of the gain narrowing by a spectral amplitude filter results in a lower overall nonlinearity due to the larger initial pulse duration. Proper spectral filtering prior amplification can dramatically improve the pulse shape and minimize unwanted side-wings, as shown e.g. in [39]. We have found experimentally that removing the BPF has indeed a negative impact on the pulse shape after the power amplifier.

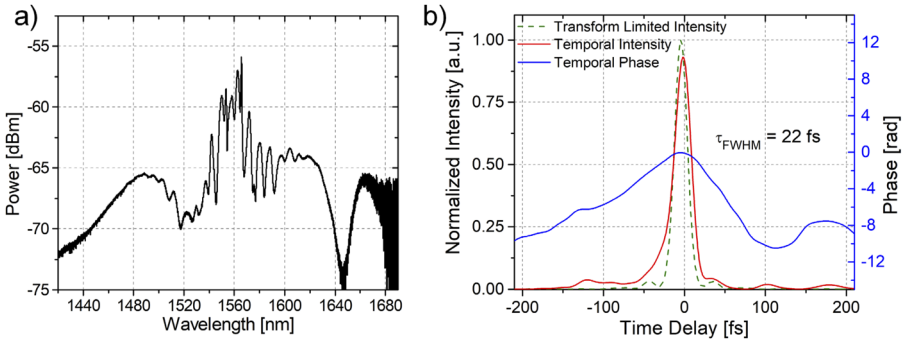

Fig. 3. (a) Optical spectrum after amplification at 1 MHz repetition rate and (b) FROG temporal intensity of the pulse (solid red line) together with the calculated transform-limited intensity (dotted green line) and temporal phase (solid blue line).

Figure 3 shows the optical spectrum and the temporal intensity of the pulse together with the temporal phase, measured via frequency-resolved optical gating technique (Mesa Photonics FS-Ultra2, FROG). Both measurements were taken at f_{rep} set to 1.02 MHz at the output of the power amplifier (second amplifier stage). In this setting, the obtained average power was 6.5 mW, which corresponds to pulse energy of approx. 6.37 nJ, more than twice than reported previously [26,27]. The energy is lower than in [33]; however, our setup has only two amplification stages in comparison to three [33], and the peak powers are comparable. The pulse duration is nearly transform-limited (22 vs. 18 fs). Further compression down to the transform limit would require additional bulk components, like prisms [25] or dispersive mirrors [16].

The ultrashort 1560 nm pulses were afterward frequency-doubled in the SHG module. The amplifier output was collimated by an aspheric lens (C220TME-C, Thorlabs) and focused by an achromatic lens (19 mm focal length, AC127-019-C-ML, Thorlabs) on a MgO:PPLN crystal (FSHNIR-ER, HC Photonics Corp.) with a 19.65 µm quasi-phase matching period and 0.3 mm poling length (L_{poled}). The SHG efficiency is at the level of 23.3%, comparable to [33]. Further optimization of the setup and increasing the conversion efficiency might be possible by using fiber-coupled PPLN crystals. The frequency-doubled beam was collimated by an aspheric lens (C560TME-B, Thorlabs) and directed through two filters: a dichroic mirror which reflects the unconverted 1560 nm pump (Thorlabs DMSP1000, Filter 1) and a band-pass filter with a cut-off at 700 nm (Thorlabs FELH0700, Filter 2) which blocks higher harmonics below 700 nm. The optical spectrum of the second harmonic and the temporal pulse intensity at f_{rep} = 1.02 MHz are presented in Figs. 4(a) and 4(b), together with the measured and retrieved FROG spectrograms (c). The spectrum is centered at 782.6 nm with a full width at half maximum (FWHM) of 19 nm. The pulse duration is 60 fs and the average power (measured after both filters) equals 1.4 mW, corresponding to a pulse energy of 1.37 nJ. It is noteworthy that the FROG measurement revealed a clean pulse shape without any pronounced sidebands and a flat temporal phase.

The used PP allows for easy repetition frequency tuning by dividing the fundamental f_{rep} by a chosen factor [35]. Figure 5(a) presents the average output power and pulse duration characteristic of the second harmonic versus repetition rate. The optical powers plotted in Fig. 5(a) are the

Biomedical Optics EXPRESS

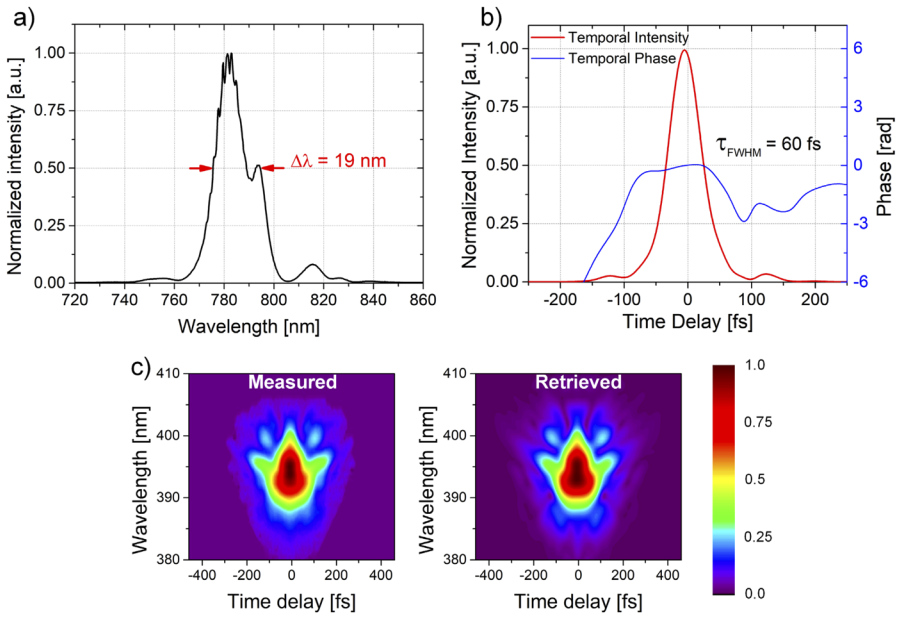

Fig. 4. (a) Generated second harmonic spectrum, (b) FROG temporal intensity of the 780 nm pulse (solid red line) together with the temporal phase (solid blue line), (c) measured and retrieved FROG spectrograms.

maximum powers that could be achieved at the given repetition rate setting (i.e., they were recorded at different amplifier pump settings). By increasing the f_{rep} from 1.02 MHz up to 11.9 MHz, we observed a linear increase of the average power (i.e., preserved pulse energy) and small changes of the pulse duration in the range of only 2 fs, which indicates that the source can be used in a wide range of frequencies with preserved pulse energy and duration, enabling optimization for specific experimental requirements (like a lifetime of fluorophores, etc.). The output power and pulse energy remain stable over long periods of time. Figure 5(b) presents the pulse energy stability measured over 6 hours without any active stabilization (only passive thermal stabilization of the oscillator, amplifiers, and PPLN crystal). It is worth noting that there is no warm-up time required to achieve the desired parameters - the system is fully turn-key operated, and the obtained stability is 0.7% rms.

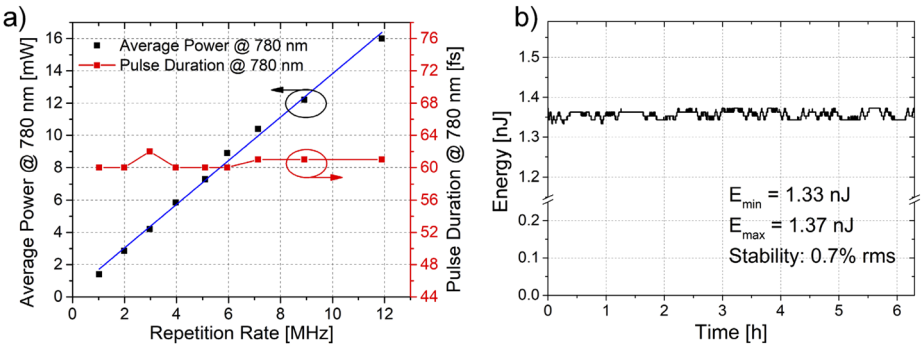

Fig. 5. (a) Measured average power and pulse duration of the 780 nm pulses as a function of the pulse repetition rate. (b) Long-term energy stability measurement over 6 hours, indicating the stability of 0.7% rms.

Biomedical Optics EXPRESS

The pulse parameters (energy, power, pulse duration) measured at each stage of the system are summarized in Table 1.

Table 1. Summary of the pulse parameters at different stages of the laser setup.

	Oscillator (f_{rep} = 35.7 MHz)	Preamplifier (f_{rep} = 35.7 MHz)	Power amplifier (f_{rep} = 1.02 MHz)	SHG module (f_{rep} = 1.02 MHz)
Pulse duration	325 fs	273 fs	22 fs	60 fs
Average power	1.1 mW	10.7 mW	6.5 mW	1.4 mW
Pulse energy	0.03 nJ	0.3 nJ	6.37 nJ	1.37 nJ

3. Application to TPEF microscopy

To verify the laser applicability to nonlinear imaging and confirm the expected effect of decreasing the pulse repetition rate, the laser was coupled to a home-build TPEF microscope schematically shown in Fig. 6(a). A variable neutral density (ND) filter placed in front of the microscope allows us to adjust the average power level at the sample. Next, the beam is directed to the galvanometer scanning system (Thorlabs GVS002), then through a scan lens (Thorlabs AC254-50-B-ML) and tube lens (Thorlabs AC254-100-B-ML) to a microscope objective (Olympus LUCPlanFL 40x/0.6 NA). The microscope objective was slightly underfilled to compromise the resolution and power efficiency. The emitted fluorescence is collected in epi-mode in a descanned manner. We use a dichroic mirror (Semrock HC 705 LP) to separate fluorescence from excitation light and a set of two additional optical filters (Semrock 694/SP BrightLine HC). The fluorescence light is collected and processed by a photon-counting GaAsP photomultiplier module (Hamamatsu H7422-40P), photon counting module (Hamamatsu C9744), data acquisition card (National Instruments USB-6212), and a custom-written LabView software. In most cases, the autofluorescence was used as a contrast. To facilitate imaging with low excitation power, the images were acquired with 40 µs dwell time and 512×512 pixels, resulting in 0.1 frames/s. To improve the signal to noise ratio, 10 frames were typically collected for averaging; however, this was not mandatory to obtain high-quality, informative images. In the case of stained samples, 10 µs dwell time was used, resulting in a 0.4 frame rate. The fluorescence intensity is quantified as a mean count of photons per pixel (mpc) within the image.

The fluorescence intensity depends on the number of absorbed photon pairs per second (N_a) in the two-photon process [8,10]:

$$N_a \propto \frac{1}{f_{rep}} \cdot \frac{\delta}{A^2 \tau} \cdot P_{avr}^2, \tag{1}$$

where f_{rep} is the pulse repetition rate, δ is the two-photon absorption cross-section, A is the spot size of the beam in focus, τ is the pulse duration (in the sample plane), and P_{avr} is the average excitation power. According to this relationship, it is possible to increase the fluorescence signal by decreasing the pulse repetition rate, if the average power at the sample is maintained at the same, unchanged level. We tested this relation by measuring the fluorescence of a fluorescence test target (Edmund Optics, #57-894) as a function of power for pulse repetition rates of 9, 3, and 1 MHz. In all cases, slopes of linear regression in log-log plot are ~1.8 [see Fig. 6(b)], indicating a second-order nonlinear process with a small contribution of linear absorption, possibly originating from a broad absorption spectrum of the test target. It is also visible that the fluorescence intensity gradually increases with decreased pulse repetition rate (with respect to 9 MHz – 2.73 times for 3 MHz and 9.34 times for 1 MHz repetition rate).

Next, we applied the developed laser and two-photon microscope for *ex vivo* imaging the cross-section of the unstained albino rat skin sample. Figures 7(a)–7(f) shows six representative TPEF images recorded at various pulse repetition rates and two average power levels. The variable

Biomedical Optics EXPRESS

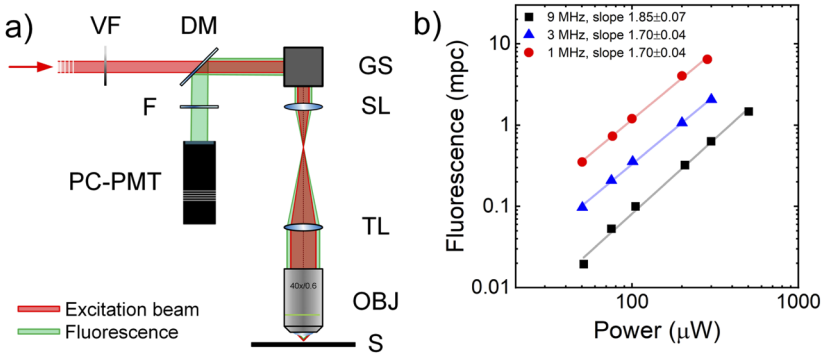

Fig. 6. (a) Experimental setup of a home-built TPEF microscope. VF – variable neutral density filter, DM – dichroic mirror, GS – galvanometer scanning unit, SL – scan lens, TL – tube lens, OBJ – objective lens, S – sample, F – cut-off filter, PC-PMT – photon-counting photomultiplier. (b) Fluorescence of test target in mean photon counts per pixel (mpc) as a function of average excitation power for 1, 3, and 9 MHz pulse repetition rates. Slopes of linear regression lines through the data points on the log-log plot indicate a two-photon process for all pulse repetition rates.

ND filter was adjusted to obtain desired average excitation power for a given pulse repetition rate, i.e., to have sufficiently bright images and yet not to saturate the PMT or the photon counter. Each image is showing the same location within the sample displaying oval structures of hair follicles. It is apparent that reducing the repetition rate to 1 MHz results in a brighter image. For quantitative analysis, we recorded the fluorescence intensity as a function of power for 9, 3, and 1 MHz repetition rates and plotted in Fig. 7(g). A quadratic function ($y = C{\cdot}x^2$) was fitted to each measurement series. We obtained 3.56 times higher value of C parameter for 3 MHz repetition rate with respect to 9 MHz, while 9.40 times higher when reducing to 1 MHz. This means that it is possible to obtain the same fluorescence intensity with 1 MHz excitation using $9.40^{1/2} = 3.07$ times less power when compared with 9 MHz excitation, which reduces the thermal damage probability [8]. Minor deviation from theoretically expected values of C parameters (3 and 9 for 3 MHz and 1 MHz pulse repetition rates, respectively) is caused by small differences in pulse duration for different repetition rates, as seen in Fig. 5. For further analysis, we recorded the fluorescence intensity as a function of the repetition rate without adjusting the variable ND filter. In this experiment, a constant pulse energy of 65 pJ in the sample plane is maintained, while the average power increases with the repetition rate. The fluorescence intensity grows linearly, as expected, and is shown in Fig. 7(h). Figure 7(i) shows the TPEF image of the sample obtained with 1 MHz and 440 μW of excitation power in the larger field of view of 600×600 μm. Summarizing, this demonstrates that the laser is performing according to expectations and can be used for imaging with various pulse repetition rates.

As another example, various biological samples were imaged with 1 MHz pulse repetition rate excitation using their endogenous autofluorescence or staining. Figure 8(a) shows the cross-section of a frog liver on a prepared microscope slide obtained with 380 μW excitation power. A characteristic structure of hepatocyte cells is visible. An example of stained sample is shown in Fig. 8(b). A cross-section of *Epipremnum scindapsus* stalk stained with rhodamine B was imaged with 750 μW of excitation power. Figures 8(c) and 8(d) show the autofluorescence image of freshly picked plant leaf of *Chamaedorea elegans* and *Epipremnum scindapsus*, respectively. In both cases, the excitation power was less than 200 μW in the sample plane. The fluorescence is originating from chlorophyll stored in the chloroplasts. All in all, it demonstrates that it is

Biomedical Optics EXPRESS

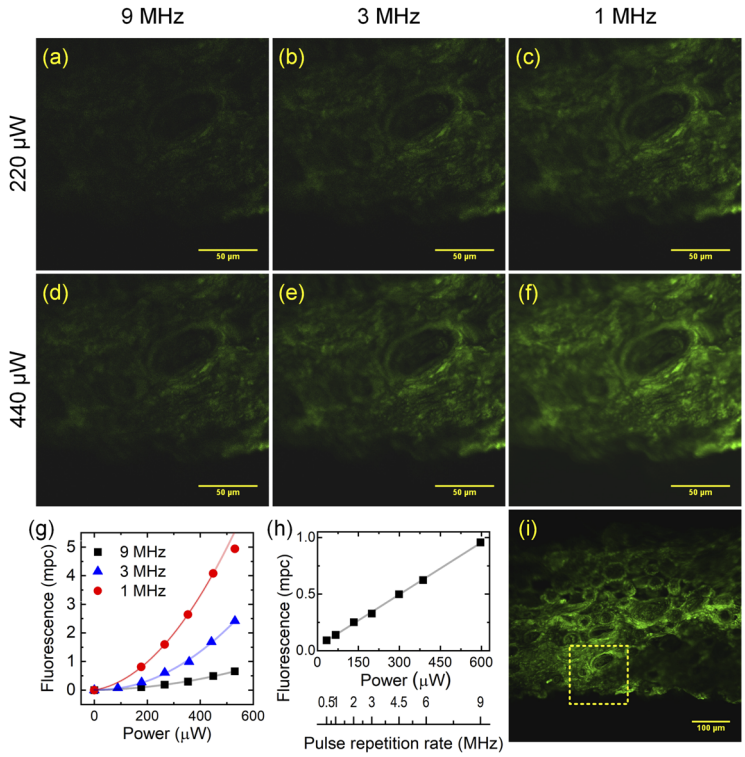

Fig. 7. Reducing the pulse repetition rate while maintaining the average excitation power allows increasing fluorescence intensity from *ex vivo* rat skin samples. (a)-(c) Imaging with 220 µW excitation power and 9, 3, and 1 MHz repetition rates. (d)-(f) Imaging with 440 µW excitation power and 9, 3, and 1 MHz repetition rates. (g) Fluorescence intensity of *ex vivo* rat skin in mean photon counts per pixel (mpc) as a function of average excitation power for 1, 3, and 9 MHz repetition rates; the last point in 1 MHz data series deviates from fit function due to saturation of photon counting electronics. (h) Fluorescence intensity of rat skin as a function of pulse repetition rate (excitation power) and maintained pulse peak power. (i) Image with a larger field of view obtained with 1 MHz repetition and 440 µW excitation power; selected ROI indicates sample region where (a)-(f) images were taken.

Biomedical Optics EXPRESS

possible to benefit from an adjustable repetition rate of the laser source for low excitation power imaging of biological samples.

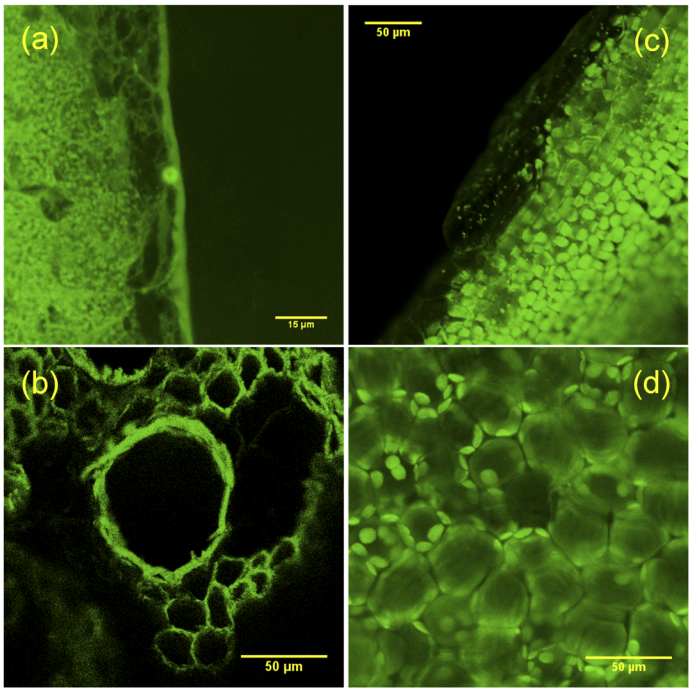

Fig. 8. Exemplary TPEF images of biological samples obtained with 1 MHz pulse repetition rate. (a) *Ex vivo* frog liver cross-section imaged with 380 µW excitation power. (b) Cross-section of *Epipremnum scindapsus* stalk stained with rhodamine B imaged with 750 µW excitation power. (c) *Chamaedorea elegans* leaf imaged with 115 µW excitation power. (d) *Epipremnum scindapsus* leaf imaged with 154 µW excitation power.

4. Summary

In conclusion, we report an exceptionally simple and compact system for low power, efficient two-photon excited fluorescence microscopy with a fiber laser source of ultrashort pulses at 780 nm wavelength. The light source is based on a frequency-doubled Er-doped fiber laser with a built-in pulse-picker for an easy repetition rate adjustment. New set-up enables easy repetition rate tuning in the range of 1 to 12 MHz, with preserved sub-65 fs pulse duration (60 fs at shortest) and energy exceeding 1.3 nJ. The performed experiments at various biological samples confirm that the light source meets the requirements of two-photon excited fluorescence microscopy, and it is possible to benefit from an adjustable pulse repetition rate. As an example, we showed that it is possible to increase the TPEF signal by 9.4 times by reducing the repetition rate from 9 to 1 MHz with maintained average power level. Moreover, our laser system can be an excellent platform for the development of an adaptive excitation source for high-speed imaging of neuronal activity [40]. We believe that such robust and reliable fiber-based sources can replace Ti:Sapphire lasers as excitation sources in outside-laboratory applications.

Biomedical Optics EXPRESS

Funding

Fundacja na rzecz Nauki Polskiej (First TEAM/2017-4/39, MAB/2019/12, POIR.04.04.00-00-3D47/16-00); Horizon 2020 Framework Programme (666295); Ministerstwo Nauki i Szkolnictwa Wyższego (International co-financed project 2016-2019 no. 3544).

Acknowledgments

We thank Maciej Popenda and Bogusław Szczupak from Wrocław University of Science and Technology for providing the 780 nm pulse autocorrelator for preliminary measurements. We acknowledge the invaluable help of Piotr Ciąćka in LabView programming, also Jadwiga Milkiewicz and Łukasz Kornaszewski (Institute of Physical Chemistry PAS) for helpful discussions. We thank Hubert Doleżyczek from Nencki Institute of Experimental Biology for the preparation of rat skin samples.

Disclosures

The authors declare no conflicts of interest.

References

1. E. Hoover and J. Squier, "Advances in multiphoton microscopy technology," Nat. Photonics **7**(2), 93–101 (2013).
2. Y. Ozeki, W. Umemura, Y. Otsuka, S. Satoh, H. Hashimoto, K. Sumimura, N. Nishizawa, K. Fukui, and K. Itoh, "High-speed molecular spectral imaging of tissue with stimulated Raman scattering," Nat. Photonics **6**(12), 845–851 (2012).
3. W. Denk, J. H. Strickler, and W. W. Webb, "Two-photon laser scanning fluorescence microscopy," Science **248**(4951), 73–76 (1990).
4. G. Palczewska, P. Stremplewski, S. Suh, N. Alexander, D. Salom, Z. Dong, D. Ruminski, E. H. Choi, A. E. Sears, T. S. Kern, M. Wojtkowski, and K. Palczewski, "Two-photon imaging of the mammalian retina with ultrafast pulsing laser," JCI Insight **3**(17), e121555 (2018).
5. A. Dvornikov, L. Malacrida, and E. Gratton, "The DIVER Microscope for Imaging in Scattering Media," Methods Protoc. **2**(2), 53 (2019).
6. D. J. Wahl, M. J. Ju, Y. Jian, and M. V. Sarunic, "Non-invasive cellular-resolution retinal imaging with two-photon excited fluorescence," Biomed. Opt. Express **10**(9), 4859–4873 (2019).
7. E. Sitiwin, M. C. Madigan, E. Gratton, S. Cherepanoff, R. M. Conway, R. Whan, and A. Macmillan, "Shedding light on melanins within in situ human eye melanocytes using 2-photon microscopy profiling techniques," Sci. Rep. **9**(1), 18585 (2019).
8. B. R. Masters, P. T. C. So, C. Buehler, N. P. Barry, J. D. B. Sutin, W. W. Mantulin, and E. Gratton, "Mitigating thermal mechanical damage potential during two-photon dermal imaging," J. Biomed. Opt. **9**(6), 1265–1270 (2004).
9. K. Teuchner, W. Freyer, D. Leupold, A. Volkmer, D. J. S. Birch, P. Altmeyer, M. Stucker, and K. Hoffmann, "Femtosecond Two-photon Excited Fluorescence of Melanin," Photochem. Photobiol. **70**(2), 146–151 (1999).
10. P. G. Antal and R. Szipőcs, "Tunable, low-repetition-rate, cost-efficient femtosecond Ti:sapphire laser for nonlinear microscopy," Appl. Phys. B **107**(1), 17–22 (2012).
11. K. Charan, B. Li, M. Wang, C. P. Lin, and C. Xu, "Fiber-based tunable repetition rate source for deep tissue two-photon fluorescence microscopy," Biomed. Opt. Express **9**(5), 2304–2311 (2018).
12. G. Donnert, C. Eggeling, and S. W. Hell, "Major signal increase in fluorescence microscopy through dark-state relaxation," Nat. Methods **4**(1), 81–86 (2007).
13. V. Sytsma and G. De Grauw, "Time-gated fluorescence lifetime imaging and microvolume spectroscopy using two-photon excitation," J. Microsc. **191**(1), 39–51 (2008).
14. C. Hille, M. Lahn, H. G. Löhmannsröben, and C. Dosche, "Two-photon fluorescence lifetime imaging of intracellular chloride in cockroach salivary glands," Photochem. Photobiol. Sci. **8**(3), 319–327 (2009).
15. C. J. de Grauw and H. C. Gerritsen, "Multiple Time-Gate Module for Fluorescence Lifetime Imaging," Appl. Spectrosc. **55**(6), 670–678 (2001).
16. R. Herda and A. Zach, "Generation of 32-fs pulses at 780 nm by frequency doubling the solitonically-compressed output of an Erbium-doped fiber-laser system," in *Conference on Lasers and Electro-Optics 2012*, OSA Technical Digest (online) (Optical Society of America, 2012), paper CTh1N.4.
17. D. Y. Tang and L. M. Zhao, "Generation of 47-fs pulses directly from an erbium-doped fiber laser," Opt. Lett. **32**(1), 41–43 (2007).
18. D. Deng, L. Zhan, Z. Gu, Y. Gu, and Y. Xia, "55-fs pulse generation without wave-breaking from an all-fiber Erbium-doped ring laser," Opt. Express **17**(6), 4284–4288 (2009).
19. Z. Q. Wang, L. Zhan, X. Fang, C. X. Gao, and K. Qian, "Generation of sub-60 fs similaritons at 1.6 μm from an all-fiber er-doped laser," J. Lightwave Technol. **34**(17), 4128–4134 (2016).

Biomedical Optics EXPRESS

20. Y. Matsui, M. D. Pelusi, and A. Suzuki, "Generation of 20-fs optical pulses from a gain-switched laser diode by a four-stage soliton compression technique," IEEE Photonics Technol. Lett. **11**(10), 1217–1219 (1999).
21. M. Tsuchiya, K. Igarashi, R. Yatsu, K. Taira, K. Y. Koay, and M. Kishi, "Sub-100 fs SDPF optical soliton compressor for diode laser pulses," Opt. Quantum Electron. **33**(7/10), 751–766 (2001).
22. Y.-T. Lin and G.-R. Lin, "Dual-stage soliton compression of a selfstarted additive pulse mode-locked erbium-doped fiber laser for 48 fs pulse generation," Opt. Lett. **31**(10), 1382–1384 (2006).
23. B. Kibler, C. Billet, P.-A. Lacourt, R. Ferriere, and J. Dudley, "All-fiber source of 20-fs pulses at 1550 nm using two-stage linear-nonlinear compression of parabolic similaritons," IEEE Photonics Technol. Lett. **18**(17), 1831–1833 (2006).
24. N. Nishizawa, "Ultrashort pulse fiber lasers and their applications," Jpn. J. Appl. Phys. **53**(9), 090101 (2014).
25. K. Kieu, R. J. Jones, and N. Peyghambarian, "Generation of few-cycle pulses from an amplified carbon nanotube mode-locked fiber laser system," IEEE Photonics Technol. Lett. **22**(20), 1521–1523 (2010).
26. H. Luo, L. Zhan, L. Zhang, Z. Wang, C. Gao, and X. Fang, ""Generation of 22.7-fs 2.8-nJ Pulses from an Erbium-Doped All-Fiber Laser Via Single-Stage Soliton Compression," J. Lightwave Technol. **35**(17), 3780–3784 (2017).
27. J. Sotor and G. Sobon, "24 fs and 3 nJ pulse generation from a simple, all polarization maintaining Er-doped fiber laser," Laser Phys. Lett. **13**(12), 125102 (2016).
28. X. Peng, K. Kim, M. Mielke, S. Jennings, G. Masor, D. Stohl, A. Chavez-Pirson, D. T. Nguyen, D. Rhonehouse, J. Zong, D. Churin, and N. Peyghambarian, "Monolithic fiber chirped pulse amplification system for millijoule femtosecond pulse generation at 1.55 μm," Opt. Express **22**(3), 2459–2464 (2014).
29. S. Han, H. Jang, S. Kim, Y.-J. Kim, and S.-W. Kim, ",MW peak power Er/Yb-doped fiber femtosecond laser amplifier at 1.5 μm center wavelength," Laser Phys. Lett. **14**(8), 080002 (2017).
30. S. Pavlova, H. Rezaei, I. Pavlov, H. Kalaycıoğlu, and F. Ömer Ilday, "Generation of 2-μJ 410-fs pulses from a single-mode chirped-pulse fiber laser operating at 1550 nm," Appl. Phys. B **124**(10), 201 (2018).
31. Z. Liu, W. Zong, Y. Liu, L. Zuo, C. Wen, T. Jiang, J. Zhang, Y. Ma, Z. Zhang, L. Chen, and A. Wang, "High Power 780 nm Femtosecond Fiber Laser," in *CLEO: 2015*, OSA Technical Digest (online) (Optical Society of America, 2015), paper AM1J.6.
32. W. Yang, D. Wu, G. Liu, B. Chen, L. Feng, Z. Zhang, and A. Wang, "256 MHz, 1 W 780 nm femtosecond fiber laser for two-photon microscopy," in *CLEO Pacific Rim Conference 2018*, OSA Technical Digest (Optical Society of America, 2018), paper Th4A.2.
33. S. Boivinet, P. Morin, J. P. Yehouessi, S. Vidal, G. Machinet, and J. Boullet, "3.5nJ femtosecond pulses at 792 nm generated by frequency doubling of an all-PM fiber high energy 48 fs laser," Proc. SPIE **10897**, 108971J (2019).
34. L. Huang, X. Zhou, Q. Liu, C. E. MacAulay, and S. Tang, "Miniaturized multimodal multiphoton microscope for simultaneous two-photon and three-photon imaging with a dual-wavelength Er-doped fiber laser," Biomed. Opt. Express **11**(2), 624–635 (2020).
35. A. Głuszek, G. Soboń, and J. Sotor, "Fast, universal, and fully automatic pulse-picker unit for femtosecond laser systems," Proc. SPIE **10974**, 1097407 (2018).
36. R. H. Stolen and C. Lin, "Self-phase-modulation in silica optical fibers," Phys. Rev. A **17**(4), 1448–1453 (1978).
37. M. D. Perry, T. Ditmire, and B. C. Stuart, "Self-phasemodulation in chirped-pulse amplification," Opt. Lett. **19**(24), 2149–2151 (1994).
38. L. Kuznetsova, A. Chong, and F. W. Wise, "Interplay of nonlinearity and gain shaping in femtosecond fiber amplifiers," Opt. Lett. **31**(17), 2640–2642 (2006).
39. T. Schreiber, D. Schimpf, D. Müller, F. Röser, J. Limpert, and A. Tünnermann, "Influence of pulse shape in self-phase-modulation-limited chirped pulse fiber amplifier systems," J. Opt. Soc. Am. B **24**(8), 1809–1814 (2007).
40. B. Li, C. Wu, M. Wang, K. Charan, and C. Xu, "An adaptive excitation source for high-speed multiphoton microscopy," Nat. Methods **17**(2), 163–166 (2020).